

Spin injection and spin dynamics at the CuPc/GaAs interface studied with ultraviolet photoemission spectroscopy and two-photon photoemission spectroscopy

Huanjun Ding and Yongli Gao

Department of Physics and Astronomy, University of Rochester, Rochester, New York 14627, USA

Mirko Cinchetti,* Jan-Peter Wüstenberg, Marina Sánchez-Albaneda, Oleksiy Andreyev, Michael Bauer, and Martin Aeschlimann

Department of Physics and Research Center OPTIMAS, University of Kaiserslautern, Kaiserslautern 67663, Germany

(Received 23 November 2007; revised manuscript received 19 May 2008; published 13 August 2008)

Interface formation between *p*-type GaAs(100) and the organic semiconductor copper phthalocyanine (CuPc) has been studied with ultraviolet photoemission spectroscopy and two-photon photoemission spectroscopy (2PPE). Spin-resolved 2PPE measurements show a highly efficient spin injection of hot electrons from GaAs into CuPc, demonstrating that spin-polarized electrons originating from the GaAs substrate can be injected into CuPc without any substantial spin-flip scattering at the interface. Furthermore, spin- and time-resolved 2PPE measurements are employed to study the temporal evolution of the spin polarization injected into the organic layer in the range up to 1 ps after injection from the GaAs substrate. The results show that the degree of spin polarization of electrons injected through the GaAs/CuPc interface into molecular orbitals just above the lowest unoccupied molecular orbital onset of CuPc is preserved longer than the spin polarization of electrons injected in energetically higher lying states.

DOI: [10.1103/PhysRevB.78.075311](https://doi.org/10.1103/PhysRevB.78.075311)

PACS number(s): 79.60.Fr, 78.47.J-, 72.25.-b, 85.75.-d

I. INTRODUCTION

Since the discovery of the giant magnetoresistive effect (GMR) in 1988, there has been extensive interest in the development of spin-based electronics.¹⁻³ Instead of using only the electrical charge of the carriers, as in traditional electronic devices, the spin degree of freedom of the mobile charge carriers is employed to carry the information in spintronics devices. Several potential advantages of spintronics devices over the conventional semiconductor devices can be expected, such as high data processing speed, low power consumption, nonvolatility, and mechanical flexibility. Some of the essential issues for the successful incorporation of spin into the existing semiconductor technology include efficient spin injection through a heterojunction and transport over distances that are comparable to the device dimensions without loss of the spin polarization, which is most commonly defined experimentally by the normalized difference between the numbers of electrons with opposite spin projections along a given direction in space.

Novel magnetoresistive devices using semiconductor spacer materials are generally based on ferromagnetic injectors,⁴⁻⁶ which provide convenient sources of spin-polarized electrons for conventional spin injection via Schottky contacts. Only recently, direct electrical spin injection with organic semiconductors (OSCs) has been demonstrated at room temperature by Dediu *et al.*⁷ Motivated by this, Xiong *et al.*⁸ obtained an impressive spin-valve effect with a trilayered ferromagnet/OSC/ferromagnet structure. A similar observation on carbon nanotubes was also reported by Tsukagoshi *et al.*⁹ At the same time, theoretical calculations of ferromagnetic metal/conjugated polymer interfaces suggest that there can be spin-density polarization in the polymer near the interface, which decays into the polymer for about six times the lattice constant of the polymer.¹⁰ The

application of organic semiconductors in spintronics devices opens great opportunities for tuning the magnetic properties by molecular design. Moreover, since organic semiconductors usually consist of elements with small atomic numbers, such as carbon and hydrogen, intrinsically weak spin-orbit coupling is expected. This leads to long spin-polarization relaxation times¹¹ that are particularly important for spintronics devices.¹²

In an organic-based spintronics device, spin-polarized electrons have to be injected from an active medium (AM) through the AM/organic interface. As a consequence, the efficiency of the spin injection at such interface is a fundamental issue to be addressed in order to understand the mechanisms influencing the device performance. The choice of the AM is an important issue as well. The AM is the source of spin-polarized carriers and its electronic structure will crucially influence the efficiency of spin injection across the specific AM/organic interface.

In this paper, we report our studies of spin injection from *p*-type GaAs(100) into CuPc. GaAs is an important inorganic semiconductor that is widely used for optoelectronics and well known for the high spin polarization that can be generated with circularly polarized light.¹³ The energy-level alignment of the GaAs(100)/CuPc interface is first investigated by ultraviolet photoemission spectroscopy (UPS). Spin-resolved two-photon photoemission spectroscopy (SR-2PPE) is used to investigate the efficiency of spin injection across the CuPc/GaAs(100) interface and spin transport in CuPc. Highly efficient spin injection of hot electrons from GaAs into CuPc is achieved, demonstrating that spin-polarized electrons originating from the GaAs substrate can be injected into CuPc without any substantial spin-flip scattering at the interface. For an advanced characterization of our system, we apply spin- and time-resolved 2PPE (STR-2PPE), giving access to the dynamics of spin-polarization relaxation with

femtosecond time resolution. The results show that the degree of spin polarization of electrons injected through the GaAs/CuPc interface into molecular orbitals just above the lowest unoccupied molecular orbital (LUMO) onset of CuPc is preserved longer than the spin polarization of electrons injected in energetically higher lying states. The gathered information about the system GaAs/CuPc may be extremely relevant for the implementation of CuPc in organic-based spintronics devices.

II. EXPERIMENT

The experiments were performed in two ultrahigh vacuum (UHV) systems. The UPS studies were done using a VG ESCA laboratory system equipped with a He I (21.2 eV) gas discharge lamp. The UHV system consists of a spectrometer chamber and an evaporation chamber, in which samples can be prepared in ultrahigh vacuum and transferred directly into the spectrometer chamber. The base pressure of the spectrometer chamber is typically 8×10^{-11} torr. The UPS spectra were recorded by using unfiltered He I excitation (21.2 eV) as a light source, with the samples biased at -5.0 V to observe the true low-energy secondary cutoff. The typical instrumental resolution for UPS measurements ranges from ~ 0.03 to 0.1 eV with photon energy dispersion of less than 20 meV.

In the 2PPE experimental setup, a femtosecond Ti:Sapphire laser is used, delivering 18 fs sech^2 temporal shaped pulses of up to 10 nJ/pulse at a repetition rate of 76 MHz. The fundamental output is linearly polarized and delivers pulses at a central wavelength of 795 nm corresponding to photon energies of 1.56 eV. A fraction of the light is frequency doubled in a 0.2-mm-thick β barium-borate crystal (BBO), leading to a probe photon energy of 3.12 eV. The fundamental (pump) pulse is circularly polarized by a quarter-wave plate, whereas the frequency-doubled (probe) pulse remains linearly p polarized. The two pulses are delayed with respect to each other using a mechanical delay stage, and can be focused onto the sample, which is mounted in an UHV chamber with a base pressure below 8×10^{-11} torr. As long as the pump and probe pulses are spatially and temporally superimposed, the high peak intensity of the laser pulses enables two-photon photoemission of electrons from the surface as a result of a two-photon absorption process, in which an electron can be emitted by absorbing just one photon from each pulse. The photoemitted electrons are analyzed by a commercial cylindrical sector analyzer (Focus CSA 300) equipped with an additional electron-spin polarization detector based on spin-polarized low-energy electron diffraction (Focus-SPLEED). The resolution of the energy analyzer was set to roughly 100 meV for the spin-integrated measurements and 150 meV for the spin-resolved (SR) measurements. In the STR-2PPE, the pump and probe pulses are separated in time by an adjustable time delay. In this case, an electron excited from the first pulse can only absorb a photon from the second pulse as long as the inelastic lifetime of the intermediate state populated by the pump exceeds the delay. The combination of spin and time resolution makes STR-2PPE a powerful technique to

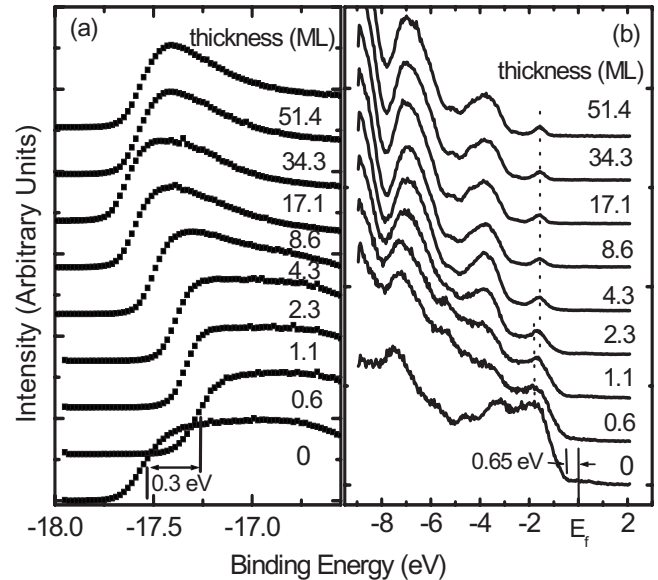


FIG. 1. UPS measurement of the (a) cutoff and (b) HOMO region of the CuPc/GaAs (100) interface as a function of CuPc coverage. The surface of GaAs was treated with Cesium prior to CuPc deposition to lower the work function. Binding energy relative to the Fermi level (E_f) is used in the figure. In Fig. 1(b), dashed lines indicate the spectral features corresponding to GaAs (left dashed line) and CuPc (right dashed line).

gain information about the spin-dependent population dynamics of the two intermediate states used in the two-step process of 2PPE, as described in more detail in Refs. 14 and 15.

A p -type GaAs(100) wafer with Zn doping concentration of $1.8 \times 10^{18} \text{ cm}^{-3}$ was cleaned by successive application of acetone, isopropanol, and de-ionized water. The sample was then etched in the solution of $\text{H}_2\text{SO}_4:\text{H}_2\text{O}_2:\text{H}_2\text{O}=3:1:1$ for 30 s and then immediately transferred into the UHV chamber to prevent reoxidation of the surface. Afterwards, the GaAs substrate was heated inside the UHV for several hours at around 430 °C. Prior to the evaporation of CuPc, the sample was treated with a small amount of cesium to reduce the work function.¹⁶ CuPc was thermally evaporated inside a side chamber attached to the main chamber with a base pressure of less than 2×10^{-9} torr. The evaporation rate of the organic film was controlled by a quartz balance. The nominal monolayer (ML) thickness of CuPc was estimated to be 3.5 Å, although epitaxial growth is not implied. All measurements were performed at room temperature.

III. ENERGY LEVEL ALIGNMENT AT THE INTERFACE

In order to understand the energy-level alignment at the CuPc/GaAs interface, UPS measurements were carried out. The low-energy secondary cutoff [Fig. 1(a)] and the highest occupied molecular orbital (HOMO) [Fig. 1(b)] of the CuPc/GaAs interface region are presented in Fig. 1 as a function of the CuPc coverage θ . All spectra are plotted in the binding-energy scale relative to the Fermi level. The negative binding energy indicates energy levels below the Fermi level. For

p-type GaAs(100), a band bending of around 0.36 eV is expected at the interface. Prior to CuPc deposition, the GaAs substrate was treated with a small amount of cesium, leading to a reduced work function of 3.64 eV and a band bending of 0.65 eV. After an initial CuPc deposition, the cutoff shifts abruptly toward the high kinetic-energy side, presumably due to the charge transfer from Cs to the first layer of CuPc. An interface dipole of about 0.3 eV can be deduced from the cut-off shift at the first monolayer of CuPc coverage. As more CuPc is evaporated onto the surface, the cutoff starts to shift back and finally becomes saturated at $\theta > 17$ ML. The final work function turns out to be the same as the one of the cesiated GaAs surface. In the HOMO region, the feature of GaAs is attenuated quickly and the feature of CuPc emerges with further deposition. For $\theta < 4$ ML, the spectra show a combination of contributions from both GaAs and CuPc. However, neither spectrum shows any discernible shift at the interface. The GaAs substrate features become attenuated greatly by the deposition of CuPc, which usually suggests Frank–van Merwe or layer-by-layer growth, similar to CuPc growth on indium tin oxide.¹⁷ The HOMO features become saturated for thick CuPc films ($\theta > 17$ ML) and are identical to a previous report.¹⁸ No occupied gap states can be observed throughout the deposition process, and the CuPc HOMO remains fixed at 1.15 eV below the Fermi level, indicating a slightly *n*-doped material. The different behavior of HOMO and the cutoff introduces a modification of the ionization potential (IP) of the CuPc overlayer due to the cesiation of the GaAs substrate. The IP reduces as more CuPc is evaporated and reaches 4.8 eV at the final step $\theta = 51$ ML, which is about 0.4 eV smaller than that of the pristine CuPc film. One of the possible explanations for this is the diffusion of the Cs atoms inside the CuPc film. The final position of the cutoff, which coincides with the position of the initial cesiated surface, corroborates this suggestion. Another possible reason is the electronic structure modification resulting from a change of the molecular orientation.¹⁹ The unoccupied states, which cannot be obtained from UPS measurements, are derived by assuming a band gap of 1.43 eV for GaAs and a HOMO-LUMO gap of 1.6 eV for CuPc, respectively. The energy-level alignment of the GaAs/CuPc interface, as deduced from our UPS measurements, is presented in Fig. 2.

IV. SPIN INJECTION AND SPIN DIFFUSION IN CuPc

In the 2PPE experiments, spin-polarized carriers are created by a circularly polarized pump pulse with photon energy of 1.56 eV (in the following: red pulse), making use of the optical selection rules close to the Γ point of the GaAs substrate (“optical orientation”). Due to the large penetration depth of red light in GaAs, these electrons are excited into the conduction band that is mainly outside the band bending area. Subsequently, some of these electrons will be accelerated toward the interface in the band bending potential and finally cross the GaAs/CuPc interface to end up in *intermediate states* above the LUMO of CuPc. According to the energy-level alignment of the GaAs/CuPc interface in Fig. 2, the conduction-band minimum of GaAs lies at 0.33 eV above

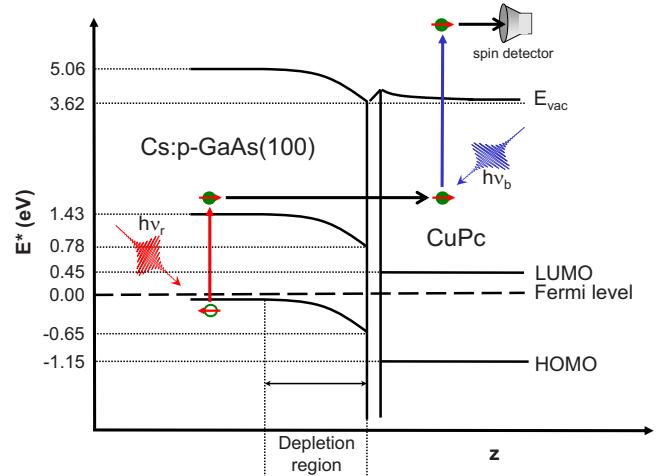


FIG. 2. (Color online) Energy-band alignment of the CuPc/GaAs interface as derived from the UPS measurements. E^* is the binding energy referenced to the Fermi energy of the system (negative values for occupied states). The excitation scheme in the STR-2PPE experiments with photon energy of 1.56 eV ($h\nu_r$) and 3.12 eV ($h\nu_b$) is also shown in the figure.

the LUMO of CuPc. This means that the electrons excited by the red pulse can easily be injected through the GaAs/CuPc interface without any barrier. The probing depth in the photoemission process is limited by the inelastic mean-free path of the electrons, which is much shorter than the light penetration depth. As a consequence, the probe pulse with photon energy of 3.12 eV (in the following: blue pulse) photoemits the electrons injected across the GaAs/CuPc interface that have reached the very surface region of CuPc (see Fig. 2). Therefore, by comparing the spin polarization of the GaAs/CuPc junction to that from the pristine GaAs substrate, we are able to investigate the spin-injection efficiency at the interface as well as the spin-relaxation processes inside the organic semiconductor after injection. In order to identify the influence of the interface on spin injection, small steps of CuPc coverage in the monolayer range have been adopted in this experiment. It is important to notice here that direct two-photon excitations from CuPc do not contribute to the 2PPE signal since the total photon energy of 4.7 eV is not sufficient to lift electrons from the HOMO level 1.15 eV below E_F beyond the vacuum level at 3.62 eV above E_F .

Figure 3 presents the spin-polarization values of the 2PPE measurements for different CuPc coverage, plotted as a function of the intermediate-state energy E^* , the binding energy (relative to the Fermi level) of the intermediate state populated by the pump pulse.²⁰ The spin-polarization curves are obtained at zero delay time (temporal overlap) between the red and blue pulses (SR-2PPE modus), so the polarized electrons generated deep in the GaAs bulk hardly have any time to redistribute in the band bending region (as a consequence of inelastic-scattering processes) as they travel almost ballistically to the interface.¹⁴ As a result, the spin polarization is higher at energies close to the bulk conduction-band minimum energy of GaAs, i.e., in the energy range 1.4 eV $< E^* < 1.6$ eV (gray shaded area in Fig. 3). For better visualization, the spin polarization that is averaged over the in-

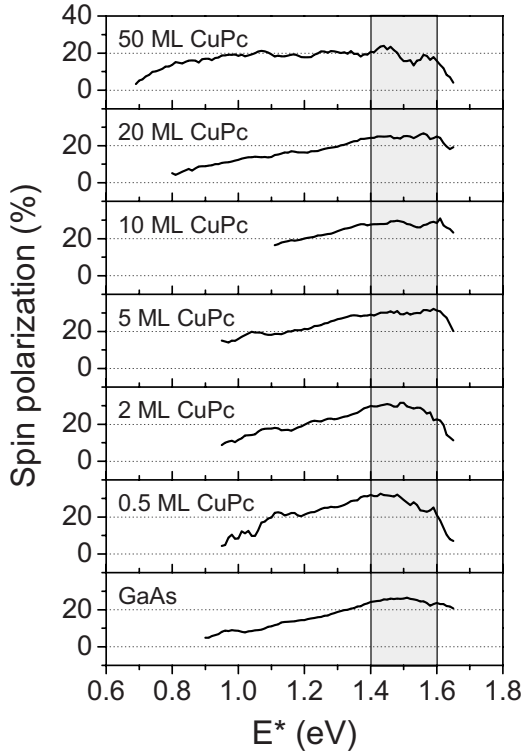


FIG. 3. Spin-polarization curves measured at room temperature by spin-resolved 2PPE for different CuPc coverage (0, 0.5, 2, 5, 10, 20, and 50 ML).

interval $1.4 \text{ eV} < E^* < 1.6 \text{ eV}$ is plotted as a function of the CuPc coverage in Fig. 4. Interestingly, the spin polarization slightly increases for initial CuPc deposition (up to 10 ML coverage). Moreover, even for the 20 ML CuPc covered GaAs sample, the spin polarization is still comparable with the initial one. This gives a direct proof for the fact that there is a negligible spin relaxation for the electrons as they are injected through the CuPc/GaAs interface into unoccupied molecular orbitals of CuPc that are lying energetically between 0.95 and 1.15 eV above the LUMO onset. The nature of the spin-enhancing effect at the interface, which has been observed in all investigated samples, is not yet completely clear. One possibility is that the charge transfer between the

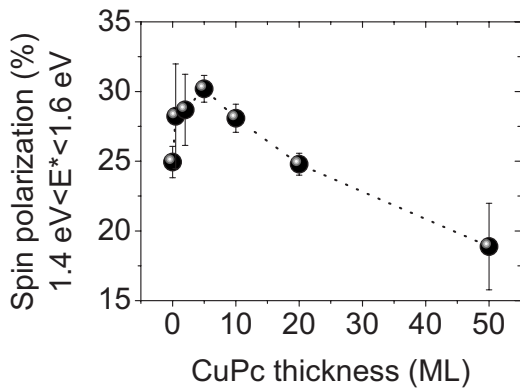


FIG. 4. Spin polarization averaged in the region $1.4 \text{ eV} < E^* < 1.6 \text{ eV}$ (gray shadowed area in Fig. 3) as a function of CuPc coverage.

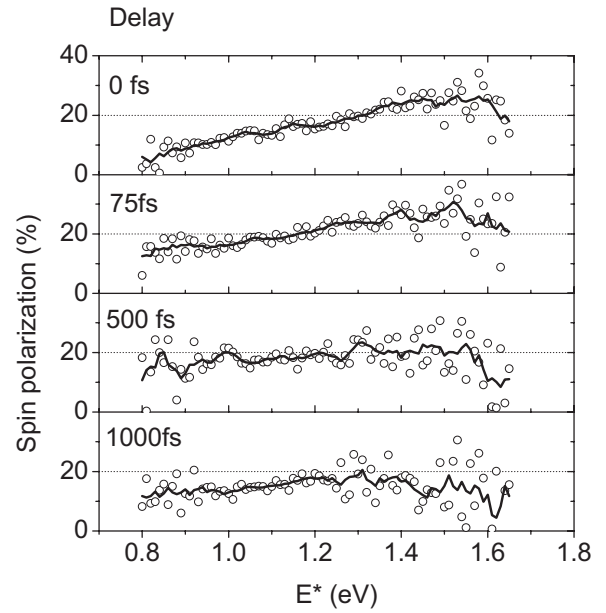


FIG. 5. Spin-polarization curves measured for 20 ML CuPc/GaAs for different pump-probe delay times. The positive delay time indicates that the red pulse pumps first, followed by the blue laser pulse as a probe.

Cs-doped GaAs and CuPc, signified by the interface dipole as shown schematically in Fig. 2, alters the spin-orbit splitting in the valence band of the GaAs surface, which in turn enhances the spin polarization. In this context, the diffusion of the Cs atoms covering the GaAs surface into the CuPc film, observed with the UPS measurements, may play an important role.

For thicker CuPc films, the polarization reduction stems from the spin-flip scattering inside the organic material, the microscopic processes determining the spin-diffusion length. In order to shed some light on the microscopic spin-flip mechanisms responsible for the spin-dependent transport in CuPc, we performed dynamical studies by means of STR-2PPE, giving access to the time dependence of the spin polarization injected in CuPc. Figure 5 shows the results of the time-resolved measurements (STR-2PPE modus) performed for the 20 ML CuPc/GaAs interface. In particular, we plot the spin polarization as a function of the intermediate-state energy E^* for different time delays between the pump (red) and the probe (blue) laser pulses. At zero time delay, when the red and blue pulses overlap in time, the spin polarization has its maximum around $E^* = 1.6 \text{ eV}$ and slowly decreases toward lower intermediate states energies. For increasing time delays, the curves become broadened and the spin polarization of higher intermediate states (i.e., states with higher energy above E_{LUMO}) decays faster than the spin polarization of low intermediate states, where the spin polarization turns out to be relatively stable. In order to make this point clear, the evolution of the spin polarization for two different energy levels at $E^* = 1.56 \text{ eV}$ and $E^* = 0.96 \text{ eV}$, respectively, is plotted in Fig. 6.

At zero delay, polarized electrons are generated in bulk GaAs in a narrow energy interval around the conduction-band minimum at $E^* = 1.46 \text{ eV}$ and have hardly any time to

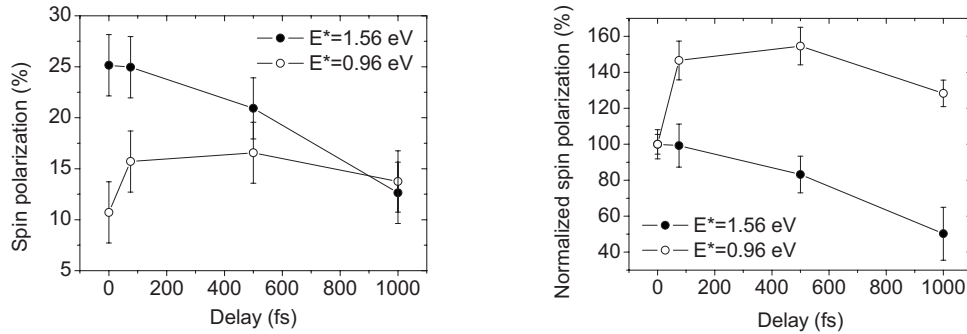


FIG. 6. Left panel: Time dependence of the spin polarization at two different intermediate states ($E^* = 1.56$ eV and $E^* = 0.96$ eV, respectively) measured for the 20 ML CuPc/GaAs interface. The data points have been obtained by integrating the data presented in Fig. 5 in an interval of ± 0.2 eV around the chosen value. Right panel: Same as left panel but with values of the spin polarization normalized to the value at zero delay.

redistribute in the band bending region. As a consequence, the spin polarization in the higher intermediate state at 1.56 eV (closer to the conduction-band minimum) is higher than in the lower intermediate state. For increasing time delay, the spin polarization in the higher intermediate state starts to decay due to elastic and quasielastic spin-flip processes and reaches after 1 ps 50% of the initial value (see the normalized spin polarization in Fig. 6—right panel). In the lower intermediate state, the spin polarization is not maximal at zero delay, instead it increases as the delay time is slightly prolonged. This is due to the well-known fact that at zero delay, the red and the blue pulses overlap in time and, hence, both possible bichromatic transitions (red blue and blue red) contribute to the yield. Blue-red transitions, however, create only unpolarized electrons in GaAs, therefore, reducing the measured spin polarization. By increasing the time delay between red and blue (positive delay here means that blue comes after red), unpolarized blue-red transitions become irrelevant, resulting in an increase in the spin polarization of the detected electrons.^{14,15} Contrary to the behavior in the high intermediate state, we observe that by increasing the delay time even longer, the spin polarization in the low intermediate state stays almost constant over the measured range of 1 ps. Thus, we can conclude that in order to achieve high efficiency in organic-based spintronics devices based on CuPc, injection of spin-polarized electrons energetically close to the LUMO onset of CuPc should be implemented by a careful choice of the bias potential.

V. CONCLUSIONS

To conclude, we have investigated the formation of the GaAs/CuPc interface by means of UPS, giving information about the energy-level alignment between the inorganic and organic semiconductor. Spin injection at the interface and spin transport into CuPc have been studied with spin- and time-resolved 2PPE spectroscopy. We have found that spin-polarized electrons created in GaAs by means of optical orientation can be injected into CuPc without any substantial spin-flip scattering at the interface, which would destroy—or at least reduce—the degree of spin polarization injected into CuPc. Furthermore, the spin polarization of electrons injected into molecular orbitals that are lying just above the LUMO onset of CuPc is preserved longer than the spin polarization of the electrons injected in states with higher energy above the LUMO. The relevance of our studies for potential applications in the field of organic-based spintronics has been discussed.

ACKNOWLEDGMENTS

This work was supported in part by the NSF under Grant No. DMR-0602870 and by DFG Research Grant No. AE 19/8-2. One of us (H.D.) acknowledges support from the DAAD/RISE program.

*cinchett@rhrk.uni-kl.de

¹S. A. Wolf, D. D. Awschalom, R. A. Buhrman, J. M. Daughton, S. vonMolnar, M. L. Roukes, A. Y. Chtchelkanova, and D. M. Treger, *Science* **294**, 1488 (2001).

²G. A. Prinz, *Science* **282**, 1660 (1998).

³I. Zutic, L. Fabian, and S. D. Sarma, *Rev. Mod. Phys.* **76**, 323 (2004).

⁴H. J. Zhu, M. Ramsteiner, H. Kostial, M. Wassermeier, H. P. Schonherr, and K. H. Ploog, *Phys. Rev. Lett.* **87**, 016601 (2001).

⁵M. Tanaka, *Semicond. Sci. Technol.* **17**, 327 (2002).

⁶A. T. Hanbicki, B. T. Jonker, G. Itskos, G. Kioseoglou, and A. Petrou, *Appl. Phys. Lett.* **80**, 1240 (2002).

⁷V. Dediu, M. Murgia, F. C. Matarotta, C. Taliani, and S. Barbanera, *Solid State Commun.* **122**, 181 (2002).

⁸Z. H. Xiong, D. Wu, Z. V. Vardeny, and J. Shi, *Nature (London)* **427**, 821 (2004).

⁹K. Tsukagoshi, B. W. Alphenaar, and H. Ago, *Nature (London)* **401**, 572 (1999).

¹⁰S. J. Xie, K. H. Ahn, D. L. Smith, A. R. Bishop, and A. Saxena,

- Phys. Rev. B **67**, 125202 (2003).
- ¹¹S. Pramanik, C.-G. Stefanita, S. Patibandla, S. Bandyopadhyay, K. Garre, N. Harth, and M. Cahay, *Nat. Nanotechnol.* **2**, 216 (2007).
- ¹²S. Sanvito, *Nat. Mater.* **6**, 803 (2007).
- ¹³F. Meier and B. P. Zakharchenya, *Optical Orientation*, Modern Problems in Condensed Matter Sciences Vol. 8 (North-Holland, Amsterdam, 1984).
- ¹⁴H. C. Schneider, J. P. Wüstenberg, O. Andreyev, K. Hiebbner, L. Guo, J. Lange, L. Schreiber, B. Beschoten, M. Bauer, and M. Aeschlimann, *Phys. Rev. B* **73**, 081302(R) (2006).
- ¹⁵M. Aeschlimann, T. Ohms, K. Hiebbner, and H. C. Schneider, in *Spin Dynamics in Confined Magnetic Structures*, Topics in Applied Physics Vol. 101, edited by B. Hillebrands and A. Thiaville (Springer, Berlin, 2006), pp. 309–340.
- ¹⁶T. Balasubramanian, J. Cao, and Y. Gao, *J. Vac. Sci. Technol. A* **10**, 3158 (1992).
- ¹⁷E. W. Forsythe, M. A. Abkowitz, Y. Gao, and C. W. Tang, *J. Vac. Sci. Technol. A* **18**, 1869 (2000).
- ¹⁸Y. Gao and L. Yan, *Chem. Phys. Lett.* **380**, 451 (2003).
- ¹⁹H. Yamane, Y. Yabuuchi, H. Fukagawa, S. Kera, K. K. Okudaira, and N. Ueno, *J. Appl. Phys.* **99**, 093705 (2006).
- ²⁰Since the spin polarization is created by the red pulse only, we consider the intermediate state energy E^* of electrons excited first by the red pulse and subsequently photoemitted by the blue pulse.